analytical chemistry

Article

pubs.acs.org/ac

Smart Vesicle Kit for In Situ Monitoring of Intracellular Telomerase Activity Using a Telomerase-Responsive Probe

Ruocan Qian,[†] Lin Ding,[†] Liwen Yan, Manfei Lin, and Huangxian Ju*

State Key Laboratory of Analytical Chemistry for Life Science, School of Chemistry and Chemical Engineering, Nanjing University, Nanjing 210093, P. R. China

Supporting Information

ABSTRACT: A smart vesicle kit was designed for in situ imaging and detection of cytoplasmic telomerase activity. The vesicle kit contained a telomerase primer (TSP) and a Cy5-tagged molecular beacon (MB) functionalized gold nanoparticle probe, which were encapsulated in liposome for intracellular delivery. After the vesicle kit was transfected into cytoplasm, the released TSP could be extended in the presence of telomerase to produce a telomeric repeated sequence at the 3′ end, which was just complementary with the loop of MB assembled on probe surface. Thus, the MB was opened upon hybridization to switch the fluorescent state from "off" to "on". The fluorescence signal depended on telomerase activity, leading to a novel strategy for in situ imaging and quantitative detection of the cytoplasmic telomerase activity. The cytoplasmic telomerase activity was estimated to be 3.2×10^{-11}, 2.4×10^{-11}, and 8.6×10^{-13} IU in each HeLa, BEL tumor and QSG normal cell, respectively, demonstrating the capability of this approach to distinguish tumor from normal cells. The proposed method could be employed for dynamic monitoring of the cytoplasmic telomerase activity in response to a telomerase-based drug, suggesting the potential application in discovery and screening of telomerase-targeted anticancer drugs.

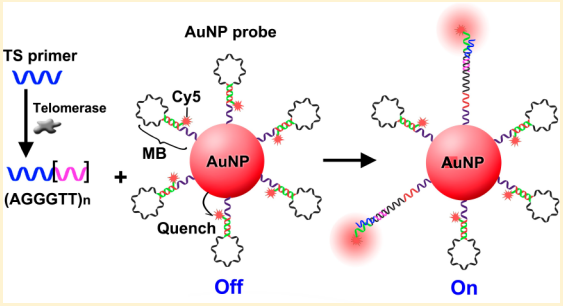

Telomeres are special functional complexes composed of tandem repeated DNA sequences at the ends of the chromosomes to protect them from deterioration during cell division process.[1−3] In normal cells, telomeres are shortened during each round of cell division, leading to cell senescence and finally cell apoptosis.[4,5] However, in cancer cells, the length of telomeres can be maintained because of the activation of telomerase.[6,7] Human telomerase is a ribonucleoprotein complex comprising a template RNA and protein, which functions as a reverse transcriptase, adding TTAGGG hexamer repeats to the end of telomeres through its RNA template.[8,9] A strong association between telomerase activity and malignancy has been found in almost all types of cancer.[10−13] Thus, telomerase can be used as a diagnostic and prognostic marker, and meanwhile it can serve as a promising target for cancer therapy.[14−18]

Owing to the significance of telomerase in cancer mechanism and therapeutic research, a variety of strategies have been reported for detection of telomerase activity, including polymerase chain reaction (PCR)-based telomeric repeat amplification protocol (TRAP),[19−21] telomeric G-quadruplex structure-based optical detection,[22] electrochemical assay,[23−26] and nanoparticle-based methods.[27−29] Most of these methods use cell extracts as detection samples and are unsuitable for in situ analysis and dynamic monitoring of intracellular telomerase activity. Focusing on the urgent need for in situ analysis of intracellular telomerase, our previous work designed a mesoporous silica nanoprobe by using telomerase-controlled primer DNA to seal fluorescein in the mesopores.[30] However, the surface adsorption of primer DNA was susceptible to surrounding environment, leading to nonspecific release of fluorescein to produce a certain degree of background.

In view of the excellent performance of AuNPs,[31−36] this work used Cy5-tagged molecular beacon (MB) functionalized gold nanoparticles (AuNPs) to design a novel probe. By coencapsulating the probe and a telomerase primer (TSP) in liposome,[37] a smart vesicle kit was thus proposed for in situ quantification and dynamic monitoring of intracellular telomerase activity (Scheme 1). The MB was a hairpin shaped DNA sequence designed to form a stem-loop structure and tagged with fluorophore Cy5, whose fluorescence could be quenched by AuNPs via fluorescence resonance energy transfer (FRET).[38] In the presence of telomerase and dNTPs, the 3′ end of TSP could be elongated to generate telomere repeat sequences. The extended part was just complementary with the loop of MB and thus could open the hairpin and release the Cy5 away from the surface of AuNPs, which turned "on" the fluorescence (Scheme 1a).

Using human cervical cells (HeLa) as a model, the TSP and probe encapsulated liposome could be efficiently delivered into cytoplasm to release the probe and TSP. The recovery of Cy5 fluorescent signal depended on cytoplasmic telomerase activity (Scheme 1b), which enabled in situ quantitative detection of

Received: April 21, 2014
Accepted: August 17, 2014
Published: August 17, 2014

   dx.doi.org/10.1021/ac502538w | *Anal. Chem.* 2014, 86, 8642−8648

Scheme 1. Schematic Illustration of Intracellular Analysis of Telomerase with MB Functionalized AuNP Probe and TSP Co-Encapsulated Liposome (Vesicle Kit)[a]

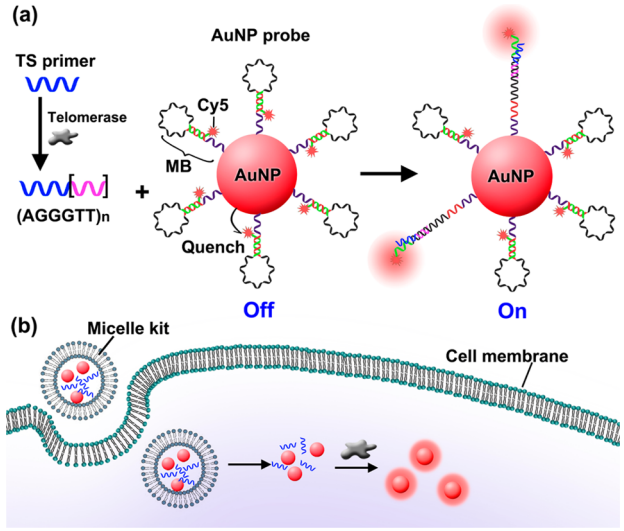

[a](a) Telomerase-triggered TSP elongation and following fluorescence recovery of probe. (b) Internalization of vesicle kit for in situ detection of telomerase.

intracellular telomerase activity at the single cell level. The vesicle kit took the advantages of the high delivery efficiency of liposome, the DNA protection function, and distance-dependent fluorescent quenching effect of AuNPs, as well as the specific recognition of MB, and provided an integrated platform for noninvasive tracking of cytoplasmic telomerase activity. The proposed strategy was simple and displayed good performance for distinguishing tumor cells from normal cells, dynamic monitoring of the telomerase response to a model drug, which demonstrated its potential application in cancer diagnosis, therapy, and telomerase-targeted drug screening.

EXPERIMENTAL SECTION

Materials and Reagents. Chloroauric acid ($HAuCl_4 \cdot 4H_2O$) was obtained from Shanghai Chemical Reagent Company (Shanghai, China). Trisodium citrate was obtained from Sinopharm Chemical Reagent Co., Ltd. (China). Epigallocatechin gallate (EGCG), 3-[(3-cholamidopropyl)-dimethylammonio]-1-propanesulfonic acid (CHAPS), ethylene glycol-bis(β-aminoethyl ether)-*N*,*N*,*N*′,*N*′-tetraacetic acid (EGTA), and phenylmethylsulfonyl fluoride (PMSF) were purchased from Sigma-Aldrich Inc. Lipofectamine-2000 (Lipo-2000) was obtained from Invitrogen China Limited. The telomerase ELISA kit was from Innovation Beyond Limits (Germany), which contained a bottle of telomerase standard solution (80 IU L^{-1}). DAPI detection kit, DNase I endonuclease, 3-(4,5-dimethylthiazol-2-yl)-2-diphenyltetrazolium bromide (MTT), dNTPs, HeLa, and Bel-7402 cells were from KeyGen Biotech. Co. Ltd. (Nanjing, China). QSG-7701 cells were from K&KM Biotech. Co. Ltd. (Wuxi, China). Gel electrophoresis loading buffer was purchased from Solarbio. Co. Ltd. (Beijing, China). Phosphate buffer saline (PBS, pH 7.4) contained 136.7 mM NaCl, 2.7 mM KCl, 8.72 mM Na_2HPO_4, and 1.41 mM KH_2PO_4. All other reagents were of analytical grade. All aqueous solutions were prepared using ultrapure water (≥18 MΩ, Milli-Q, Millipore).

RNase A and all DNA sequences were purchased from Sangon Biological Engineering Technology & Co. Ltd. (Shanghai, China) with the following sequences:

Molecular beacon (MB): 5′-HS-$(AAA\ AAA)_3$ TCT AGC CCC TAA CCC TAA CCC TAA GCT AGA-Cy5-3′

Telomerase primer (TSP): 5′-AAT CCG TCG AGC AGA GTT-3′

Control DNA (O1): 5′-$(AAA\ AAA)_3$-3′

Apparatus. The transmission electron microscopic (TEM) images were obtained on a JEM-2100 transmission electron microscope (JEOL Ltd., Japan). Dynamic light scattering (DLS) was observed on a 90 Plus/BI-MAS equipment (Brookhaven). Zeta potential analysis was performed on a Zetasizer (Nano-Z, Malvern, U.K.). The UV−vis absorption spectra were obtained with a UV−vis spectrophotometer (Nanodrop-2000C, Nanodrop). Gel electrophoresis was performed on the DYCP-31 BN electrophoresis analyzer (Liuyi Instrument Company, China) and imaged on the Biorad ChemDoc XRS. Flow cytometric analysis was performed on a Coulter FC-500 flow cytometer (Beckman-Coulter). The fluorescence spectra were obtained on a spectrofluorophotometer (RF-5301PC, Shimadzu, Japan). The cell images were gained on a TCS SP5 laser scanning confocal microscope (Leica, Germany). Telomerase ELISA kit and MTT assay were performed on a microplate reader (680, Bio-Rad).

Preparation of MB-Functionalized AuNPs. AuNPs were prepared according to the previous report.[39] After heating 200 mL of $HAuCl_4$ solution (0.01%) to 100 °C, 5.0 mL of trisodium citrate (1%) was added quickly to the boiling solution under continuous stirring. The reaction mixture was stirred at 100 °C for 1 h until the color turned deep red and then stored at 4 °C. A volume of 10 μL of Cy5-tagged MB (100 μM) was then added to 1 mL of AuNP solution and stirred at room temperature overnight. Afterward, 0.1 mL of PBS containing 2 M NaCl was added to the mixture stepwise for stabilizing the obtained AuNP probe, which was centrifuged and washed with PBS twice, then resuspensed in 1 mL of PBS. The supernatant containing excess Cy5-tagged MB was collected for fluorescent analysis.

Preparation of TSP and Probe Co-Encapsulated Liposome. Liposomal vesicle was used to deliver the probe and TSP into cells. A volume of 20 μL of as-prepared probe solution and 10 μL of TSP (100 μM) were mixed with 20 μL of serum-free medium, while 0.5 μL of Lipo-2000 was dissolved in 20 μL of serum-free medium and incubated for 5 min. After two solutions were mixed and incubated for 20 min at room temperature, the TSP and probe coencapsulated liposome as the vesicle kit could be formed. The probe and O1 coencapsulated liposome was also prepared for control with the same procedure.

Gel Electrophoresis. Samples 1 and 2 were prepared by incubating the mixture of 10 μL of TSP (100 μM) and 10 μL of dNTPs (10 mM each) with 10 μL of cell extract or 10 μL of telomerase (40 IU L^{-1}) at 37 °C for 1 h. Samples 3 and 4 were prepared by incubating the mixture of 10 μL of MB (100 μM), 10 μL of TSP (100 μM), and 10 μL of dNTPs (10 mM each) with 10 μL of cell extract or 10 μL of telomerase (40 IU L^{-1}) at 37 °C for 1 h.

The gel electrophoresis was performed by adding 7.5 μL of TSP solution (100 μM), sample 1, sample 2, MB solution (100 μM), sample 3, sample 4, and ladder DNA solution (10 μM) as indicators in the mixture of 1.5 μL of loading buffer and 1.5 μL of GelRed, respectively, and then injecting these mixtures into a

dx.doi.org/10.1021/ac502538w | Anal. Chem. 2014, 86, 8642−8648

10% polyacrylamide hydrogel in tris-borate-EDTA (TBE) buffer. Electrophoresis was carried out at 100 V in TBE buffer for 1 h. The resulting board was observed under UV irradiation.

Cell Culture. HeLa cells were cultured in a flask in Dulbecco's modified Eagle's medium (DMEM, GIBCO) supplemented with 10% fetal calf serum (FCS, Sigma), penicillin (100 μg mL^{-1}), and streptomycin (100 μg mL^{-1}) at 37 °C in a humidified chamber, containing 5% CO_2. BEL-7402 and QSG-7701 cells were, respectively, cultured in a flask in RPMI-1640 (GIBCO) supplemented with 10% FCS, penicillin (100 μg mL^{-1}), and streptomycin (100 μg mL^{-1}) at 37 °C in a humidified atmosphere containing 5% CO_2. Cell number was determined using a Petroff-Hausser cell counter.

Detection of Telomerase Activity in Cell Extract. Cells were collected in the exponential phase of growth, and 5×10^7 cells were dispensed in a 1.5 mL EP tube, washed twice with 0.1 M ice-cold PBS (pH 7.4), and resuspended in 200 μL of ice-cold CHAPS lysis buffer containing 10 mM Tris-HCl (pH 7.5), 1 mM $MgCl_2$, 1 mM EGTA, 0.1 mM PMSF, 0.5% CHAPS, and 10% glycerol. The mixture was incubated for 30 min on ice and then centrifuged at 16 000 rpm at 4 °C for 20 min. The supernatant was collected and diluted to 200 μL for analysis or stored frozen at −80 °C.

A standard addition method was used for quantification of telomerase activity in the HeLa cell extract. After incubating the mixtures of 10 μL of cell extract (corresponding to 2.5×10^6 cells), 10 μL of TSP (100 μM), 10 μL of dNTPs (10 mM each), and 1 mL of probe in the absence and presence of 10 μL of spiked telomerase (20 IU L^{-1} from telomerase ELISA kit) at 37 °C for 1 h, the fluorescent intensity was detected, respectively. The telomerase in 10 μL of cell extract was calculated to be 7.2×10^{-5} IU, i.e., each HeLa cell contained 2.9×10^{-11} IU telomerase.

In Situ Imaging of Intracellular Telomerase Activity with Vesicle Kit. A volume of 0.5 mL of 1×10^6 mL^{-1} HeLa cells (or BEL, QSG cells) were seeded in each confocal dish for 24 h, and 70 μL of the prepared vesicle kit was then added into each cell-adhered dish. After incubation at 37 °C for different times, the cells were sent for fluorescent confocal imaging or flow cytometric detection. As a control, HeLa cells (0.5 mL, 1×10^6 mL^{-1}) were seeded in each confocal dish for 24 h and then incubated with the mixture of 20 μL of probe, 10 μL of TSP (100 μM), and 40 μL of serum-free medium at 37 °C.

The TEM image was taken after incubating HeLa cells (0.5 mL, 1×10^6 mL^{-1}) with the prepared vesicle kit of 70 μL at 37 °C for 2 h and fixed on a copper grid with 10% methanol for 1 h at 4 °C. The dynamic monitoring of intracellular telomerase activity of EGCG-treated HeLa cells was performed after the cells were treated with different amounts of EGCG in confocal dishes for 48 h and then incubated with 70 μL of the prepared vesicle kit at 37 °C for 2 h.

Quantification of Intracellular Telomerase Activity. HeLa cells treated with different amounts of EGCG displayed varied telomerase activity, thus a set of 50 μL cell extracts provided the standard samples to obtain the calibration curve for quantifying the intracellular telomerase activity. Here the EGCG-treated cells were divided into two groups. One group was transfected with 70 μL of the vesicle kit to obtain the average fluorescence intensity (FI) by confocal imaging and reading the average red channel intensity of the cell area, which was subtracted by background red channel intensity with Adobe Photoshop software. Another group was used to obtain the extracts of cells for detect the corresponding telomerase activity in a single cell (T) by ELISA kit analysis. The ELISA kit analysis was performed with a standard curve method by adding 50 μL of cell extracts in the wells of the ELISA plate to incubate at 37 °C for 30 min. The plate was washed with PBS and added with 50 μL of labeling reagent (from the kit) to incubate at 37 °C for 30 min. Afterward, the medium was removed, and 50 μL of color development agent A and 50 μL of color development agent B (from the kit) were added to vibrate for 10 min at 37 °C. A volume of 50 μL of stop buffer (from the kit) was finally added to each well to stop the color reaction, and the absorbance was measured at 450 nm on a microplate reader.

MTT Assay. The cytotoxicity of probe was tested by MTT assay. After HeLa cells (100 μL, 1.0×10^6 mL^{-1}) were seeded in the wells of 96-well plate for 4 h, the medium was discarded. The cells were then washed twice with PBS and incubated with 100 μL culture medium containing 20 μL of probe for different times. Cells incubated in culture medium were used as the control. After washing with PBS, MTT (50 μL, 1 mg mL^{-1}) was added to each well and incubated at 37 °C for 4 h, followed by discarding the medium. Then 100 μL of dimethyl sulfoxide was added to each well, and the cell plate was vibrated for 15 min at room temperature to dissolve the crystals formed by the living cells. The absorbance of each well was measured at 490 nm on a microplate reader. The relative cell viability (%) was calculated by $(A_{test}/A_{control}) \times 100\%$.

Statistical Analysis. Data were obtained from at least three biological replicates (for cell-involved experiments) with three technical replicates and were expressed as means ± standard error of mean.

RESULTS AND DISCUSSION

Characterization of AuNPs and Probe. The TEM image of the prepared AuNPs showed good distribution with an average diameter around 13 nm (Figure 1a), which was further

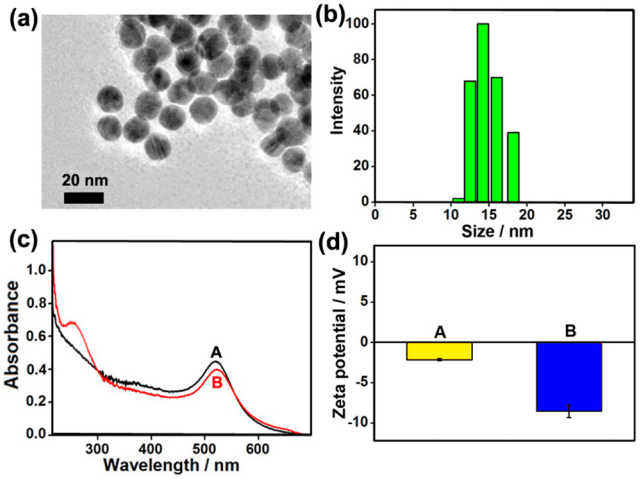

Figure 1. (a) TEM image and (b) DLS characterization of the prepared AuNPs. (c) UV−vis spectra of (A) AuNPs and (B) probe. (d) Zeta-potentials of (A) AuNPs and (B) probe in H_2O.

confirmed by DLS experiment showing an average hydration diameter of 14.2 nm (Figure 1b). The successful binding of MB to AuNPs was demonstrated by UV−vis spectra (Figure 1c) and zeta-potential analysis (Figure 1d). The UV−vis spectrum of probe showed the characteristic peaks of DNA at 260 nm and AuNPs at 522 nm. The latter displayed a small red shift compared with unmodified AuNPs at 519 nm (Figure 1c). In

dx.doi.org/10.1021/ac502538w | Anal. Chem. 2014, 86, 8642−8648

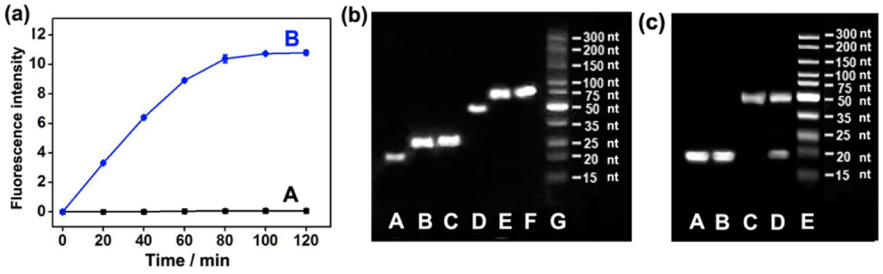

Figure 2. (a) Plot of fluorescence intensity of the probe solution (1 mL) containing TSP (10 μL, 100 μM) and dNTPs (10 μL, 10 mM each) vs incubation time in absence (A) and presence (B) of telomerase (10 μL, 40 IU L^{-1}). (b) Electrophoresis image of (A) TSP, (B) mixture of TSP, dNTPs, and HeLa cell extract after incubation for 1 h, (C) mixture of TSP, dNTPs, and telomerase after incubation for 1 h, (D) MB, (E) mixture of MB, TSP, dNTPs, and HeLa cell extract after incubation for 1 h, (F) mixture of MB, TSP, dNTPs, and telomerase after incubation for 1 h, and (G) ladder DNA. (c) Electrophoresis image of (A) TSP, (B) mixture of TSP, dNTPs, and QSG cell extract after incubation for 1 h, (C) MB, (D) mixture of MB, TSP, dNTPs, and QSG cell extract after incubation for 1 h, and (E) ladder DNA.

comparison with AuNPs, the probe presented a more negative potential (Figure 1d), indicating the conjugation of negatively charged DNA. To measure the amount of MB assembled on the probe, the standard curve was obtained with a series of MB solutions (Figure S1 in the Supporting Information). From the fluorescence intensity of the supernatant containing excess MB collected after the preparation of probe (Figure S1 in the Supporting Information, inset), the amount of MB on each probe was estimated to be around 100.[40]

Telomerase-Responsive Fluorescence Switch. To evaluate the telomerase-responsive fluorescence recovery of the probe, the fluorescence intensity of the probe (1 mL) in the presence of TSP (10 μL, 100 μM), dNTPs (10 μL, 10 mM each), and telomerase (10 μL, 40 IU L^{-1}) was observed after incubation for different times. The fluorescence intensity gradually increased with the increasing incubation time and reached a plateau after 80 min (Figure 2a), while the fluorescence intensity did not change in the absence of telomerase, demonstrating the telomerase-responsive fluorescence switch. The switch mechanism could be explained as the extension of TSP by telomerase and the subsequent hybridization between the extension product and MB, which opened the MB and led to the recovery of the initially AuNP-quenched fluorescence (Scheme 1a). The extension and hybridization could be verified by gel electrophoresis experiments (Figure 2b). After incubating TSP, dNTPs with an extract of HeLa cells or pure telomerase for 1 h at 37 °C, the products showed a wide band at 25−30 nt (Figure 2b, lanes B and C), which was about 1−2 telomere repeat segments longer than TSP (Figure 2b, lane A), verifying the recognition and elongation of TSP by telomerase. After incubating MB, TSP, and dNTPs with an extract of HeLa cells or telomerase, each lane after electrophoresis displayed a band around 80 nt (Figure 2b, lanes E and F), about 30 nt longer than pure MB (Figure 2b, lane D), which could be attributed to the hybridization of the extended TSP product with MB. In order to exclude the effect of unspecific polymerase coexisted in cell extract on the elongation of TSP, the telomerase and Hela cell extract were first pretreated with RNase A to deactivate the RNA-dependent activity of telomerase and then mixed with the probe, TSP, and dNTPs, respectively. After incubation for 1 h, the mixtures showed tiny fluorescence recovery (Figure S2a in the Supporting Information), which was only 1%−5% of the fluorescence observed without the pretreatment of RNase A, demonstrating the RNA dependency of the telomerase activity and the strict telomerase-driven TSP extension. These results were further verified by gel electrophoresis characterization (Figure S2b in the Supporting Information, lanes C and E). Note that the denatured ladder DNA and ladder DNA showed the same band location and distribution below 300 nt/bp in the gel electrophoresis image (Figure S2c in the Supporting Information), the ladder DNA was directly used as a marker for convenience. In addition, a telomerase negative cell (QSG) extract was used to perform the TSP extension and MB hybridization experiments (Figure S2c in the Supporting Information), which did not show any elongation or hybridization product and demonstrated the telomerase-dependent extension. These experiments confirmed the existence of telomerase in the extracts of cancer cells and suggested the feasibility of the proposed TSP and MB sequences for analysis of intracellular telomerase.

The fluorescence off-on switch and the stability of probe were also tested in different media (Figure S3 in the Supporting Information). Owing to the lack of salt, which is essential to telomerase-triggered TSP elongation and DNA hybridization, the fluorescence recovered much slower in water (Figure S3a in the Supporting Information). Contrarily, the time course curves in DMEM or RPMI 1640 were similar to those obtained in PBS (Figure S3b−d in the Supporting Information), excluding the interference of culture medium components on telomerase-controlled fluorescence recovery. The stability of probe in different buffers were verified by DLS detection, which showed an almost unchanged average hydration diameter after fluorescence recovery experiments (Figure S3e in the Supporting Information), indicating good stability. These experiments also suggested the adaptability of the probe in complex biological environments such as cell extract and cytoplasm.

The capability of the proposed probe for analysis of telomerase activity from the cell extract was examined by a standard addition method. From the fluorescent spectra of the incubated mixtures of cell extract, probe, TSP, and dNTPs in the presence or absence of spiked telomerase (Figure S4 in the Supporting Information), the telomerase activity in each HeLa cell was calculated to be 2.9×10^{-11} IU, which was consistent with our previous result (3.0×10^{-11} IU).[30]

Protection Ability of Probe to MB against Nuclease in Acidic pH. In cellular internalization pathways, the probe might be processed in complex acidic environments with various enzymes, thus the resistance ability of the probe against nuclease cleavage of DNase I in acidic PBS was first investigated. The probe showed negligible fluorescence

dx.doi.org/10.1021/ac502538w | Anal. Chem. 2014, 86, 8642−8648

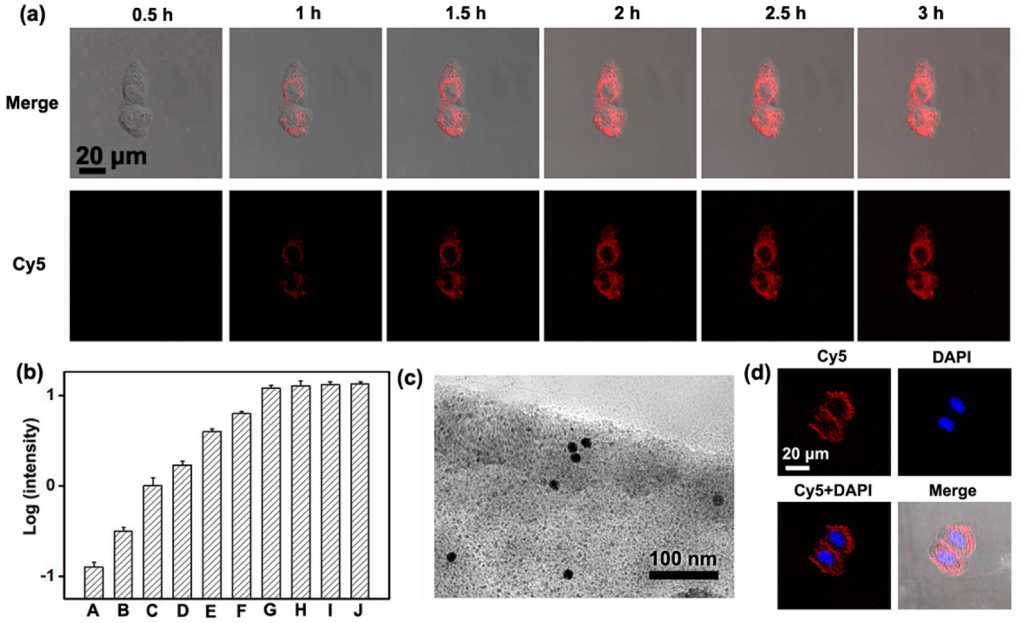

Figure 3. (a) Time course of confocal images of HeLa cells incubated with 70 μL of vesicle kit. (b) Flow cytometric detection of HeLa cells after incubation with 70 μL of vesicle kit for 0, 20, 40, 60, 80, 100, 120, 140, 160, and 180 min (from A to J), respectively. (c) TEM image of AuNP probe-internalized HeLa cell. (d) Confocal images of HeLa cells incubated with 70 μL of vesicle kit and 20 μL of DAPI staining solution for 2 h.

recovery in the presence of DNase I in pH 6.0 PBS (Figure S5 in the Supporting Information), demonstrating the protective ability of AuNP against nuclease in an acidic subcellular environment,[35,36] which ensured the intracellular usage of the probe.

In Situ Imaging of Intracellular Telomerase Activity. In order to efficiently deliver probe and TSP into cells, lipo-2000, a widely used transfection agent, was employed to coencapsulate these components, which could be released after liposome-mediated internalization. Considering the existence of dNTPs in cytoplasm,[41] there was no need to encapsulate them in Lipo-2000. The obtained vesicle could be regarded as "a smart kit" for tracking the intracellular telomerase activity by imaging operation.

The feasibility of the vesicle kit for in situ imaging of intracellular telomerase activity was investigated by dynamically observing the fluorescence of Cy5 upon the transfection of the kit (Figure 3a). In the beginning, no obvious fluorescence signal was observed within 30 min. After 1 h, weak fluorescence could be observed in the cytoplasm, and the intensity increased with the increasing incubation time (Figure 3a), which was attributed to the opening of MB by telomerase-catalyzed TSP elongation product, and thus indicated the existence of telomerase in the cytoplasm.[42] Interestingly, the strong fluorescence emission occurred around the nucleus, demonstrating higher activity of telomerase in the cytoplasm nearby the nucleus.

The fluorescence switch was also verified with flow cytometry, which was in good agreement with the confocal imaging result (Figure 3b). The optimized incubation time of 2 h was chosen. The amount of probe for preparation of the vesicle kit was also optimized to be 20 μL by flow cytometry (Figure S6 in the Supporting Information). Besides the confocal images, the internalization and localization of the probe in cytoplasm was also confirmed by TEM detection (Figure 3c) and DAPI staining with blue fluorescence (Figure 3d), which verified the presence of the probe in the cytoplasm. Thus, the proposed kit enabled the selective detection of the cytoplasmic telomerase activity. Because of the high expression of telomerase in cytoplasm of many types of cancer cells,[43] this method could be used for cancer discrimination.

To demonstrate the necessity of using lipo-2000 for intracellular delivery, a control experiment was performed using HeLa cells treated by TSP and probe without lipo-2000 (Figure S7 in the Supporting Information). In the absence of lipo-2000, no obvious fluorescence signal was observed within 1.5 h and only weak fluorescence could be observed even after 2 h, which might be attributed to much lower internalization efficiency of TSP compared with the smart vesicle kit.

Specificity for MB Opening in Living HeLa Cells. To demonstrate the specific opening of MB by the elongated TSP, a control DNA, O1, 5′-(AAA AAA)$_3$-3′, was used to replace TSP for preparation of the liposome vesicle and the same cell incubation test. After incubation with O1 and probe coencapsulated liposome for 2 h, the confocal microscopic image of HeLa cells showed little fluorescence (Figure S8 in the Supporting Information), which verified the specificity. The result suggested the specific recognition of telomerase toward TSP and the successful delivery and stable existence of TSP in cytoplasm.

Cytotoxicity of Probe. The cytotoxicity of AuNP probe was tested using MTT assay. After incubating HeLa cells with probe for different times, the absorbance was measured to calculate the relative cell viability at each time point. After treated with the probe for 3 h, the cells still maintained about 90% of the cell viability (Figure S9 in the Supporting Information), demonstrating the low cytotoxicity of the probe, which was desirable for intracellular detection.

Monitoring of Telomerase Activity in Response to Model Drug. In view of the ability of the vesicle kit, it was employed for in situ monitoring the change of intracellular telomerase activity in response to a model telomerase-inhibiting drug, EGCG.[44] After incubating HeLa cells with different amounts of EGCG in culture medium for 48 h, they were

dx.doi.org/10.1021/ac502538w | Anal. Chem. 2014, 86, 8642−8648

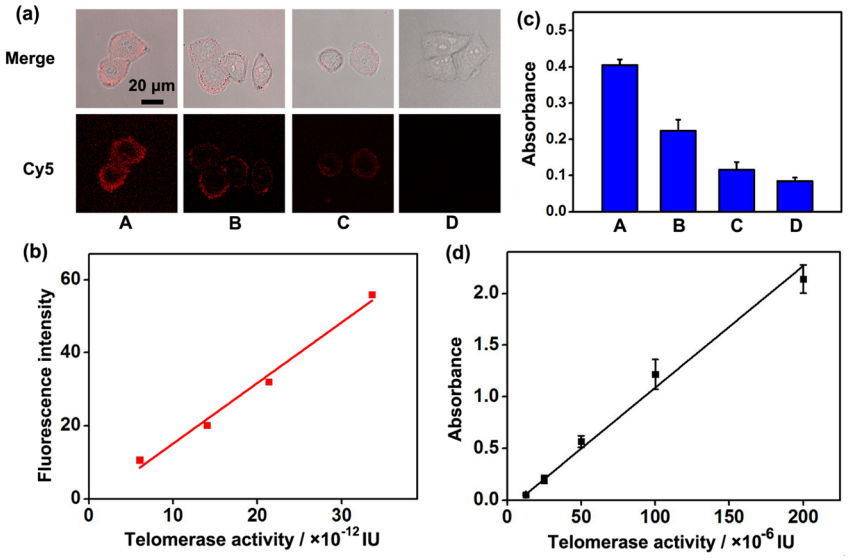

Figure 4. (a) Confocal images of HeLa cells treated with 0, 60, 120, and 250 μg mL^{-1} EGCG (from A to D) for 48 h and then 70 μL of vesicle kit for 2 h. (b) Plot of average intracellular fluorescence intensity (FI) vs telomerase activity in single cell (T). (c) Absorbance of cell extracts collected from HeLa cells treated with 0, 60, 120, and 250 μg mL^{-1} EGCG (from A to D) using telomerase ELISA kit. (d) Plot of absorbance detected with ELISA kit vs telomerase activity.

subjected to vesicle kit analysis. The fluorescence intensity decreased with the increasing EGCG amount (Figure 4a), showing the efficient inhibition ability of EGCG to telomerase activity. These results demonstrated that the vesicle kit could be used for in situ tracking of the dynamic change of intracellular telomerase activity and also suggested the potential application for discovery and screening of telomerase-targeted drugs, which would benefit the development of anticancer drugs.

Quantification of Intracellular Telomerase Activity. The feasibility of the vesicle kit for quantification of intracellular telomerase activity was further examined. The HeLa cells treated with different amounts of EGCG were used for obtaining the calibration curve by using the vesicle kit to detect the fluorescence intensity of confocal images (Figure 4a,b) and the telomerase ELISA kit to detected the telomerase activity in the cell extract (Figure 4c) with a standard curve (Figure 4d). The calibration curve of the vesicle kit for in situ quantification of intracellular telomerase activity is shown in Figure 4b, which gave a linear regression equation of FI = 0.598 + 1.66 × 10^{12} T. With this calibration curve, the telomerase activity in single HeLa cell was estimated to be 3.2 × 10^{-11} IU. This value was in good agreement with 2.9 × 10^{-11} IU detected with the cell extract and 3.0 × 10^{-11} IU in our previous report.[30]

Distinguishing Tumor Cells from Normal Cells with Vesicle Kit. The proposed vesicle kit could be used to compare the intracellular telomerase activity across different cancer and normal cell lines using BEL-7402 cells (liver cancer cells) and QSG-7701 cells (liver normal cells) as the models. Both confocal observation and flow cytometric detection indicated that BEL cells showed obviously higher telomerase activity than QSG cells (Figure 5), suggesting the correlation of cytoplasmic telomerase activity with malignancy. Using the established quantification method, the telomerase activity in single BEL and QSG cell was estimated to be 2.4 × 10^{-11} and 8.6 × 10^{-13} IU, respectively. Thus, the proposed strategy provided a facile approach for distinguishing cancer cells from normal cells.

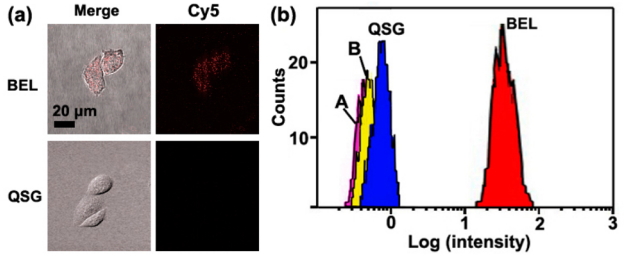

Figure 5. (a) Confocal microscopic images and (b) flow cytometric detection of BEL and QSG cells after incubation with 70 μL of vesicle kit for 2 h using (A) QSG and (B) BEL cells as the control.

CONCLUSIONS

This work designed a smart vesicle kit for in situ imaging and quantification of intracellular telomerase activity. This approach integrated the telomerase-triggered TSP elongation and a telomerase-responsive probe to realize the in situ tracking of the cytoplasmic telomerase activity with good performance. The practicality of the proposed method was demonstrated by quantifying the intracellular telomerase activity in different cell types, which could also be used for distinguishing cancer cells from normal cells with different levels of telomerase activity. This method could be further applied for dynamically monitoring of the variation of the intracellular telomerase activity in response to a telomerase-targeted drug. Compared with existing methods for telomerase activity assay, the proposed vesicle kit could perform the in situ detection through a "one step incubation" and lowered fluorescence background owing to the efficient AuNP-based FRET mechanism, thus providing an inexpensive, convenient method with high sensitivity. The strategy would accelerate the understanding of telomerase involved biological processes and provide a favorable analytical tool for cancer diagnosis, therapy, and telomerase-related drug screening.

dx.doi.org/10.1021/ac502538w | Anal. Chem. 2014, 86, 8642−8648

■ ASSOCIATED CONTENT

Supporting Information

Additional information as noted in text. This material is available free of charge via the Internet at http://pubs.acs.org.

■ AUTHOR INFORMATION

Corresponding Author

*Phone/fax: +86-25-83593593. E-mail: hxju@nju.edu.cn.

Author Contributions

†R.Q. and L.D. contributed equally to this work.

Notes

The authors declare no competing financial interest.

■ ACKNOWLEDGMENTS

This work was financially supported by the National Basic Research Program (Grants 2010CB732400 and 2014CB744501) and the National Natural Science Foundation of China (Grants 21322506, 21135002, 21121091, and 91213301).

■ REFERENCES

(1) Blackburn, E. H. *Nature* **2000**, *408*, 53.
(2) Hammond, P. W.; Cech, T. R. *Nucleic Acids Res.* **1997**, *25*, 3698.
(3) Baur, J. A.; Zou, Y.; Shay, J. W.; Wright, W. E. *Science* **2001**, *292*, 2075.
(4) Rodier, F.; Campisi, J. *J. Cell Biol.* **2011**, *192*, 547.
(5) Shay, J. W.; Wright, W. E. *Carcinogenesis* **2005**, *26*, 867.
(6) Shay, J. W.; Bacchetti, S. *J. Cancer* **1997**, *33*, 787.
(7) Masutomi, K.; Yu, E. Y.; Khurts, S. *Cell* **2003**, *114*, 241.
(8) Harley, C. B. *Nat. Rev. Cancer* **2008**, *8*, 167.
(9) Blasco, M. A. *Nat. Rev. Genet.* **2005**, *6*, 611.
(10) Mergny, J. L.; Riou, J. F.; Mailliet, P.; Teulade-Fichou, M. P.; Gilson, E. *Nucleic Acids Res.* **2002**, *30*, 839.
(11) Meyerson, M. *J. Clin. Oncol.* **2000**, *18*, 2626.
(12) Blackburn, E. H. *Mol. Cancer Res.* **2005**, *3*, 477.
(13) Shay, J. W.; Wright, W. E. *Semin. Cancer Biol.* **2011**, *21*, 349.
(14) Zhou, X. M.; Xing, D. *Chem. Soc. Rev.* **2012**, *41*, 4643.
(15) Shay, J. W.; Zou, Y.; Hlyama, E.; Wright, W. E. *Hum. Mol. Genet.* **2001**, *10*, 677.
(16) Williams, S. C. P. *Nat. Med.* **2013**, *19*, 6.
(17) Agrawal, A.; Dang, S.; Gabrani, R. *Recent Pat. Anti-Cancer Drug Discovery* **2012**, *7*, 102.
(18) Lu, L. G.; Zhang, C.; Zhu, G. J.; Irwin, M.; Risch, H.; Menato, G.; Mitidieri, M.; Katsaros, D.; Yu, H. *Breast Cancer Res.* **2011**, *13*, R56.
(19) Herbert, B. S.; Hochreiter, A. E.; Wright, W. E.; Shay, J. W. *Nat. Protoc.* **2006**, *1*, 1583.
(20) Kim, N. W.; Wu, F. *Nucleic Acids Res.* **1997**, *25*, 2595.
(21) Hou, M.; Xu, D. W.; Bjorkholm, M.; Gruber, A. *Clin. Chem.* **2001**, *47*, 519.
(22) Freeman, R.; Sharon, E.; Teller, C.; Henning, A.; Tzfati, Y.; Willner, I. *ChemBioChem* **2010**, *11*, 2362.
(23) Yang, W. Q.; Zhu, X.; Liu, Q. D.; Lin, Z. Y.; Qiu, B.; Chen, G. N. *Chem. Commun.* **2011**, *47*, 3129.
(24) Liu, J.; Lu, C. Y.; Zhou, H.; Xu, J. J.; Wang, Z. H.; Chen, H. Y. *Chem. Commun.* **2013**, *49*, 6602.
(25) Mori, K.; Sato, S.; Kodama, M.; Habu, M.; Takahashi, O.; Nishihara, T.; Tominaga, K.; Takenaka, S. *Clin. Chem.* **2013**, *59*, 289.
(26) Yi, Z.; Wang, H. B.; Chen, K.; Gao, Q.; Tang, H.; Yu, R. Q.; Chu, X. *Biosen. Bioelectron.* **2014**, *53*, 310.
(27) Patolsky, F.; Gill, R.; Weizmann, Y.; Mokari, T.; Banin, U.; Willner, I. *J. Am. Chem. Soc.* **2003**, *125*, 13918.
(28) Li, Y.; Li, X.; Ji, X. T.; Lia, X. M. *Biosens. Bioelectron.* **2011**, *26*, 4095.
(29) Wang, J. S.; Wu, L.; Ren, J. S.; Qu, X. G. *Small* **2012**, *8*, 259.
(30) Qian, R. C.; Ding, L.; Ju, H. X. *J. Am. Chem. Soc.* **2013**, *135*, 13282.
(31) Llevot, A.; Astruc, D. *Chem. Soc. Rev.* **2012**, *41*, 242.
(32) Duncan, B.; Kim, C.; Rotello, V. M. *J. Controlled Release* **2010**, *148*, 122.
(33) Li, F.; Zhang, H. Q.; Dever, B.; Li, X. F.; Le, X. C. *Bioconjugate Chem.* **2013**, *24*, 1790.
(34) Llevot, A.; Astruc, D. *Chem. Soc. Rev.* **2009**, *38*, 1759.
(35) Giljohann, D. A.; Seferos, D. S.; Patel, P. C.; Millstone, J. E.; Rosi, N. L.; Mirkin, C. A. *Nano Lett.* **2007**, *7*, 3818.
(36) Seferos, D. S.; Giljohann, D. A.; Hill, H. D.; Prigodich, A. E.; Mirkin, C. A. *J. Am. Chem. Soc.* **2007**, *129*, 15477.
(37) Dalby, B.; Cates, S.; Harris, A.; Ohki, E. C.; Tilkins, M. L.; Price, P. J.; Ciccarone, V. C. *Methods* **2004**, *33*, 95.
(38) Yun, C. S.; Javier, A.; Jennings, T.; Fisher, M.; Hira, S.; Peterson, S.; Hopkins, B.; Reich, N. O.; Strouse, G. F. *J. Am. Chem. Soc.* **2006**, *127*, 3115.
(39) Maye, M. M.; Nykypanchuk, D.; Van der Lelie, D.; Gang, O. *J. Am. Chem. Soc.* **2006**, *128*, 14020.
(40) Burda, C.; Chen, X. B.; Narayanan, R.; El-Sayed, M. A. *Chem. Rev.* **2005**, *105*, 1025.
(41) Gandhi, V. V.; Samuels, D. C. *Nucleosides, Nucleotides Nucleic Acids* **2011**, *30*, 317.
(42) Morin, G. B. *Cell* **1989**, *59*, 521.
(43) Kyo, S.; Masutomi, K.; Maida, Y.; Kanaya, T.; Yatabe, N.; Nakamura, M.; Tanaka, M.; Takarada, M.; Sugawara, I.; Murakami, S.; Taira, T.; Inoue, M. *Am. J. Pathol.* **2003**, *163*, 859.
(44) Lin, S. C.; Li, W. C.; Shih, J. W.; Hong, K. F.; Pan, Y. R.; Lin, J. J. *Cancer Lett.* **2006**, *236*, 80.